9

# Complex Coefficient IIR Digital Filters

Zlatka Nikolova, Georgi Stoyanov, Georgi Iliev and Vladimir Poulkov
*Technical University of Sofia*
*Bulgaria*

## 1. Complex Coefficient IIR Digital Filters – Basic Theory

### 1.1 Introduction

Interest in complex signal processing goes back quite some time: in 1960 Helstrom (Helstrom, 1960) and Woodward (Woodward, 1960) used the complex envelope presentation to solve problems with signal detection, as did Bello (Bello, 1963), who used it to describe time-invariant linear channels. A number of publications at that time also considered complex signal processing but on a purely theoretical basis. The concept of digital filters with complex coefficients, which will be also referred to as *complex filters*, was developed by Crystal and Ehrman (Crystal & Ehrman, 1968). This work in fact marks the beginning of interest in complex filters and is one of the most often-cited publications. It demonstrated the increased effectiveness of complex signal processing compared to real signal processing and focused the attention of researchers on that new area of science. This area subsequently progressed well, especially in telecommunications, where the complex representation of signals is very useful as it allows the simple interpretation and realization of quite complicated processing tasks, such as modulation, sampling and quantization.

Digital filters with complex coefficients have attracted great interest, owing to their advantages when processing both real and complex signals. As they have both real and imaginary inputs and outputs, the signals they process have to be likewise separated into real and imaginary parts in order to be represented as complex signals. Complex filters have been of theoretical interest for a long time but have only been the subject of intensive experimental investigation over the past two decades, thanks to the rapid development of technology. They have many areas of application, one of the most important being modern telecommunications, which very often uses narrowband signals which are complex in nature (Martin, 2003). Digital complex filters are used to generate SSB (Single Side Band) narrowband signals, typically employed in many wireless telecommunication devices, e.g. SSB transmitters and receivers, complex ΔΣ-modulators, trans-multiplexors, radio-receivers, mobile terminals etc. These devices employ processes such as complex modulation, filtering, mixing, speech analysis and synthesis, and adaptive filtering. Complex filtering is also preferred when DFT (Discrete Fourier Transform) is carried out, as it is a linear combination of complex components. This type of processing is required for high-speed wireless standards. Many of the research problems associated with complex digital filtering have been successfully solved but scientific and technological advances challenge researchers with new problems or require new and better solutions to existing problems.

In this chapter we examine IIR (Infinite Impulse Response) digital filters only. They are more difficult to synthesize but are more efficient and selective than FIR (Finite Impulse Response) filters. In general, the choice between FIR and IIR digital filters affects both the filter design process and the implementation of the filter. FIR filters are sufficient for most filtering applications, due to their two main advantages: an exact linear phase response and permanent stability.

### 1.2 Complex Signals and Complex Filters – an Overview

A complex signal is usually depicted by:

$$X(t) = A\left[\cos(\theta_C t) + j\sin(\theta_C t)\right] = Ae^{j\theta_C t} = X_R(t) + jX_I(t) \tag{1}$$

where "*R*" and "*I*" indicate real and imaginary components. The spectrum of the complex signal $X(t)$ is in the positive frequency $\theta_C$, while that of the real one $X_R(t)$ is in the frequencies $\theta_C$ and - $\theta_C$.

There are two well-known approaches to the complex representation of the signals – by inphase and quadrature components, and using the concept of analytical representation. These approaches differ in the way the imaginary part of the complex signal is formed. The first approach can be regarded as a low-frequency envelope modulation using a complex carrier signal. In the frequency domain this means linear translation of the spectrum by a step of $\theta_C$. Thus, a narrowband signal with the frequency of $\theta_C$ can be represented as an envelope (the real part of the complex signal – $X_R(t)$), multiplied by a complex exponent $e^{j\theta_C t}$, named cissoid (Crystal & Ehrman, 1968) or complexoid (Martin, 2003) (Fig. 1).

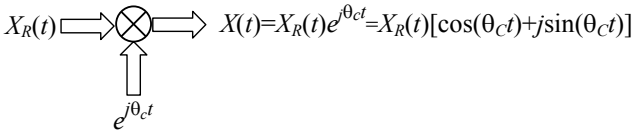


Fig. 1. Complex representation of a narrowband signal.

Analytical representation is the second basic approach to displaying complex signals. The negative frequency components are simply reduced to zero and a complex signal named *analytic* is formed. The real signal and its Hilbert transform are respectively the real and imaginary parts of the analytic signal, which occupies half of the real signal frequency band while its real and imaginary components have the same amplitude and 90° phase-shift. Analytic signals are, for example, the multiplexed OFDM (Orthogonal Frequency Division Multiplexing) symbols in wireless communication systems.

Complex signals are easily processed by complex circuits, in which complex coefficient digital filters play a special role. In contrast to real coefficient filters, their magnitude responses are not symmetric with respect to the zero frequency. A bandpass (BP) complex filter, which is arithmetically symmetric with regards to its central frequency, can be derived by linear translation with a step $\theta$ of the magnitude response of a real lowpass (LP) filter (Crystal & Ehrman, 1968). This is equivalent to applying the substitution:

$$z^{-1} \rightarrow z^{-1}e^{j\theta} = z^{-1}(\cos\theta + j\sin\theta) \tag{2}$$

to the real transfer function (also called real-prototype transfer function) thus obtaining the analytical expression of the complex transfer function:

$$H_{Real}(z) \xrightarrow{z^{-1}=z^{-1}(\cos\theta+j\sin\theta)} H_{Complex}(z) = H_R(z) + jH_I(z). \tag{3}$$

$H_{Complex}(z)$ is a transfer function with complex coefficients and with the same order of $N$ as the real prototype $H_{Real}(z)$, while its real and imaginary parts $H_R(z)$ and $H_I(z)$ are of doubled order $2N$ real coefficient transfer functions. When $H_{Real}(z)$ is an LP transfer function then $H_R(z)$ and $H_I(z)$ are of BP type. For a highpass (HP) real prototype transfer function we get $H_R(z)$ and $H_I(z)$, respectively of BP and bandstop (BS) types.
The substitution (2) is also termed "pole rotation" because it rotates the poles of the real transfer function to an angle of θ both clockwise and anti-clockwise, simultaneously doubling their number (Fig. 2).

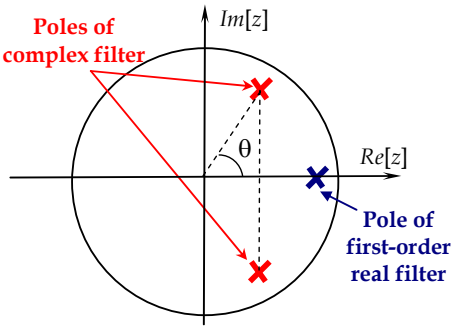


Fig. 2. Pole rotation of a first-order real transfer function after applying the substitution (2).

Starting with:

$$Y(z) = H_{Complex}(z)X(z) \tag{4}$$

and supposing that the quantities in (4) are complex, they can be represented by their real and imaginary parts:

$$Y(z) = Y_R(z) + jY_I(z); \quad X(z) = X_R(z) + jX_I(z); \quad H_{Complex}(z) = H_R(z) + jH_I(z). \tag{5}$$

Then the equation (4) becomes:

$$\begin{aligned} Y(z) &= [H_R(z) + jH_I(z)][X_R(z) + jX_I(z)] = \\ &= [H_R(z)X_R(z) - H_I(z)X_I(z)] + j[H_I(z)X_R(z) + H_R(z)X_I(z)], \end{aligned} \tag{6}$$

and its real and imaginary parts respectively are:

$$Y_R(z) = H_R(z)X_R(z) - H_I(z)X_I(z); \qquad Y_I(z) = H_I(z)X_R(z) + H_R(z)X_I(z). \tag{7}$$

According to the equations (7), the block-diagram of a complex filter will be as shown in Fig. 3.

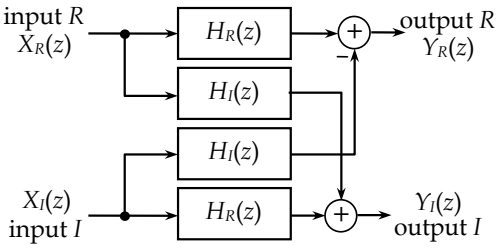


Fig. 3. Block-diagram of a complex filter.

The synthesis of a complex filter is an important procedure because its sensitivity is influenced by the derived realization. A non-canonic complex filter realization will be obtained if $H_R(z)$ and $H_I(z)$ are synthesised individually.
The process of synthesising the complex filter can be better understood by examining a particular filter realization – a real LP first-order filter section (Fig. 4a) with transfer function:

$$H_{\text{Real}}^{LP}(z) = \frac{1+z^{-1}}{1-a_1 z^{-1}}. \tag{8}$$

The complex transfer function obtained after the substitution (2) is applied to the real transfer function (8) is:

$$H_{Real}^{LP}(z) = \frac{1+z^{-1}}{1-a_1 z^{-1}} \xrightarrow{z^{-1}=z^{-1}(\cos\theta + j\sin\theta)} H_{Complex}(z) = \frac{1+\cos\theta z^{-1} + j\sin\theta z^{-1}}{1-a_1\cos\theta z^{-1} - ja_1\sin\theta z^{-1}}. \tag{9}$$

The separation of its real and imaginary parts produces:

$$H_{Complex}(z) = H_R(z) + jH_I(z) = \frac{1+(1-a_1)\cos\theta z^{-1} + a_1\sin\theta z^{-2}}{1+2a_1\cos\theta z^{-1} + a_1^2 z^{-2}} + j\frac{(1+a_1)\sin\theta z^{-1}}{1+2a_1\cos\theta z^{-1} + a_1^2 z^{-2}}. \tag{10}$$

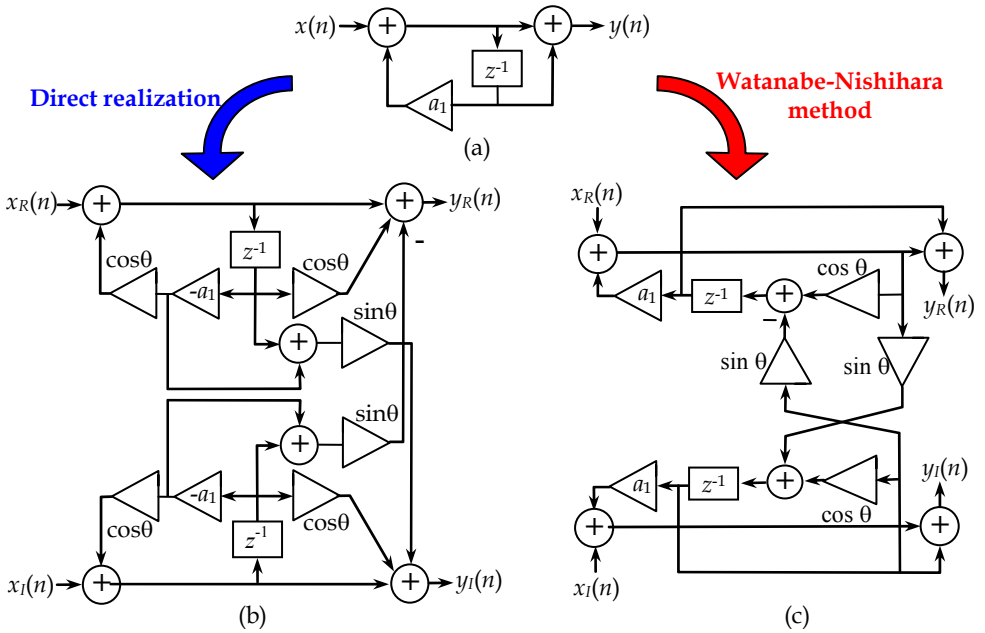


Fig. 4. Realization of (a) real LP first-order filter section; (b) direct-form complex BP filter section; (c) complex BP filter (Watanabe-Nishihara method).

The difference equation corresponding to the transfer function (9) is:

$$\begin{aligned} y_R(n)+jy_I(n)=&\left[x_R(n)+\cos\theta x_R(n-1)-\sin\theta x_I(n-1)-a_1\cos\theta y_R(n-1)+a_1\sin\theta y_I(n-1)\right]+\\ &+j\left[x_I(n)+\cos\theta x_I(n-1)+\sin\theta x_R(n-1)-a_1\cos\theta y_I(n-1)-a_1\sin\theta y_R(n-1)\right]. \end{aligned} \tag{11}$$

Direct realization of (11) leads to the structure depicted in Fig. 4b. Obviously the realization is canonic only with respect to the delays. The direct realization of complex filters is studied in some publications (Sim, 1987) although the sensitivity is not minimized.

One of the best methods for the realization of complex structures is offered by Watanabe and Nishihara (Watanabe & Nishihara, 1991). The structure of the real prototype is doubled, for the real input and output as well as for the imaginary input and output (Fig. 5). Bearing in mind that processed signals are complex, after applying the complex transformation (2) the signals after each delay unit are described as:

$$B_R=z^{-1}\left(A_R\cos\theta-A_I\sin\theta\right);\qquad B_I=z^{-1}\left(A_R\sin\theta+A_I\cos\theta\right). \tag{12}$$

Applying the Watanabe-Nishihara method to the real LP first-order filter section in Fig. 4a, the complex filter shown in Fig. 4c is derived.

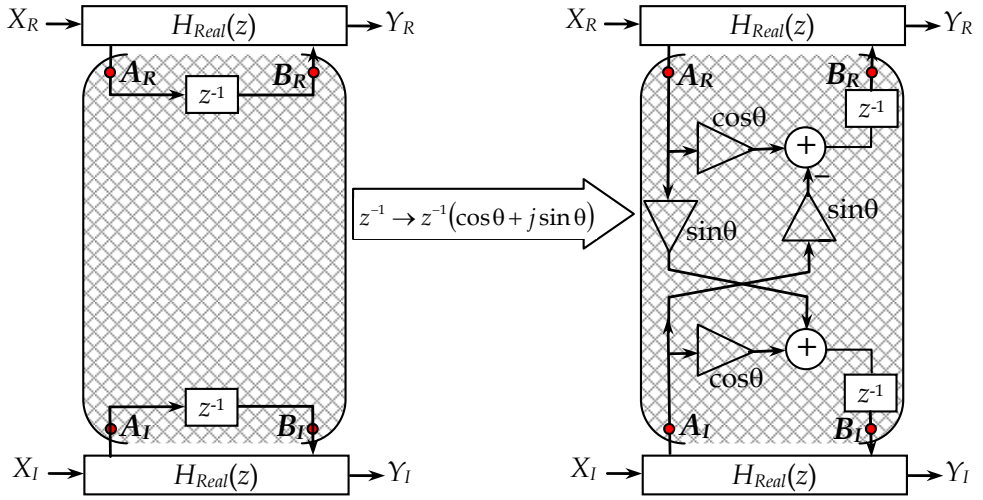


Fig. 5. Complex structure realized by Watanabe and Nishihara method.

The Watanabe-Nishihara method is universally applicable to any real structure, the complex structure obtained being canonic with respect to the multipliers and delay units if the sin- and cosin-multipliers are not counted. Moreover, the number of identical circuit transformations performed and the number of multipliers in the real filter-prototype are the same.

A special class of filters, named *orthogonal complex filters,* is derived (Sim, 1987) (Watanabe & Nishihara, 1991) (Nie et al., 1993), when θ is exactly equal to π/2 in the complex transformation (2):

$$z^{-1} = z^{-1}\left(\cos\frac{\pi}{2} + j\sin\frac{\pi}{2}\right) \text{ or } z = -jz\,. \tag{13}$$

These filters are used for narrowband signal processing. Obtained after the orthogonal transformation (13) is applied, the orthogonal complex transfer function $H(-jz)$ has alternately-changing coefficients, i.e. real and imaginary. The magnitude response of an orthogonal complex filter is symmetric with respect to the central frequency $\omega_c$, which is exactly 1/4 of the real filter's sampling frequency $\omega_s$.

### 1.3 Sensitivity Considerations

Digital filters are prone to problems from two main sources of error. The first is known as *transfer function sensitivity with respect to coefficients* and refers to the quantization of multiplier coefficients, which changes the transfer function carried out by the filter. The second source of error is *roundoff noise* due to finite arithmetical operations, which degrades the signal-to-noise ratio (SNR) at the digital filter output. These errors have been extensively discussed in the literature.

In this chapter normalized (classical or Bode) sensitivity is used to estimate how the changes of a given multiplier coefficient α influence the magnitude response of the structure:

$$S_{\alpha}^{|H(j\omega)|} = \frac{\partial |H(j\omega)|}{\partial \alpha} \frac{\alpha}{|H(j\omega)|}. \tag{14}$$

The overall sensitivity to all multiplier coefficients is evaluated using the worst-case sensitivity

$$WS_{\alpha_i}^{H(e^{j\omega})} = \sum_i \left| S_{\alpha_i}^{H(e^{j\omega})} \right|, \tag{15}$$

or the Schoefler sensitivity (SS), defined as WS but with quadratic addends (Proakis & Manolakis, 2006):

$$SS_{\alpha_i}^{H(e^{j\omega})} = \sum_i \left| S_{\alpha_i}^{H(e^{j\omega})} \right|^2. \tag{16}$$

Minimization of sensitivity is a well-studied problem but the method that is most widely used by researchers is *sensitivity minimization by coefficient conversion*. In this chapter we use Nishihara's coefficient conversion approach (Nishihara, 1980).
The sensitivity of magnitude, phase response, group-delay etc. is a function of frequency. This has to be taken into account when different digital structures are compared to each other because the sensitivity may differ in the different frequency bands. An indirect criterion for the sensitivity of a transfer function in a particular frequency band is the pole-location density in the corresponding area of the unit circle for a given word-length.
Frequency-dependent sensitivities allow different digital filter realizations to be compared to each other in a wide frequency range. For this reason, magnitude sensitivity function (14) and worst-case sensitivity (15) will mainly be considered in this work.

## 2. Orthogonal Complex IIR Digital Filters – Synthesis and Sensitivity Investigations

### 2.1 Introductory Considerations

The synthesis of orthogonal complex low-sensitivity canonic first- and second-order digital filter sections allows an efficient orthogonal cascade filter to be achieved. Such a filter can be developed using the method of approximation and design given in (Stoyanov et al., 1997). The procedure is simple in the case of arithmetically symmetric BP/BS specifications and consists of the following steps:

1. Shift the specifications along the frequency axis until the zero frequency becomes central for them.

2. Apply any possible LP or HP (for BS specifications) approximation, which produces the transfer function in a factored form.

3. Select or develop low-sensitivity canonic first- and second-order LP/HP filter sections.

4. Apply the circuit transform (13) $z^{-1} \to -jz^{-1}$ to obtain the orthogonal sections, which are used to form the desired orthogonal complex BP/BS cascade realization.

The procedure becomes a lot more difficult in the case of non-symmetric specifications. There are, however, methods of solving the problems but at the price of quite complicated mathematics and transformations (Takahashi et. al., 1992) (Martin, 2005).
The last two steps in the above-described procedure are discussed here. Some low-sensitivity canonic first- and second-order orthogonal complex BP/BS digital filter sections are developed and their low sensitivities are experimentally demonstrated.
The Watanabe-Nishihara method (Watanabe & Nishihara, 1991) is selected to develop new sections. According to this method, it is expected that the sensitivity properties of the prototype circuit will be inherited by the orthogonal circuit obtained after the transformation. Starting from that expectation, we apply the following strategy: first select or develop very low-sensitivity LP/HP prototypes for a given pole-position and then apply the orthogonal circuit transformation to derive the orthogonal complex BP/BS digital filter sections.
The selection of LP/HP first- and second-order real prototype-sections requires the following criteria to be met:

- The circuits must have canonic structures;
- The magnitude response must be unity for DC (in the case of LP transfer functions), likewise for fs/2 (in the case of HP transfer functions), thus providing zero magnitude sensitivity;
- The sensitivity must be minimized;
- Prototype sections must be free of limit cycles

### 2.2 Low-Sensitivity Orthogonal Complex IIR First- Order Filter Sections

In order to derive a narrowband orthogonal complex BP filter, a narrowband LP real filter-prototype must be used. When the orthogonal substitution is applied to an HP real prototype, the orthogonal complex filter will have both BP and BS outputs. The most advantageous approach is to employ a universal real digital filter section, which simultaneously realizes both LP and HP transfer functions.
After a comprehensive search, we selected the best two universal first-order real filter-prototype structures that meet the above-listed requirements. They are: MHNS-section (Mitra et al., 1990-a) and a low-sensitivity LS1b-structure (Fig. 6a) (Topalov & Stoyanov, 1990).
When the Watanabe-Nishihara orthogonal circuit transformation is applied to the real filter-prototypes, the orthogonal complex LS1b (Fig. 6b) and MHNS filter structures are obtained (Stoyanov et al., 1996).
After the orthogonal circuit transform (13) is applied to the LP real transfer function (18) $H_{LS1b}^{LP}(z)$ the resulting orthogonal complex transfer function $H_{LS1b-LP}(-jz)$ has complex coefficients, which are alternating real and imaginary numbers. Being a complex transfer function, it can be represented by its real and imaginary parts, which are of double order and are real coefficients:

$$H_{LS1b-LP}(-jz) = H_{LS1b-LP}^{R}(z) + jH_{LS1b-LP}^{I}(z). \tag{17}$$

Because the real prototype section is universal, i.e. has simultaneous LP and HP outputs, the orthogonal structure has two inputs – real and imaginary, and four outputs – two real ($R1$ and $R2$) and two imaginary ($I1$ and $I2$). Thus there are eight realized transfer functions, in the form of four pairs: the two parts of each pair are identical to each other and also equal to

the real and imaginary parts of the LP- and HP-based orthogonal transfer functions - (20)÷(23). Only (22) is of BS type, the rest are BP. The central frequency of an orthogonal filter $\omega_C$ is constant and is a quarter of the sampling frequency $\omega_s$.

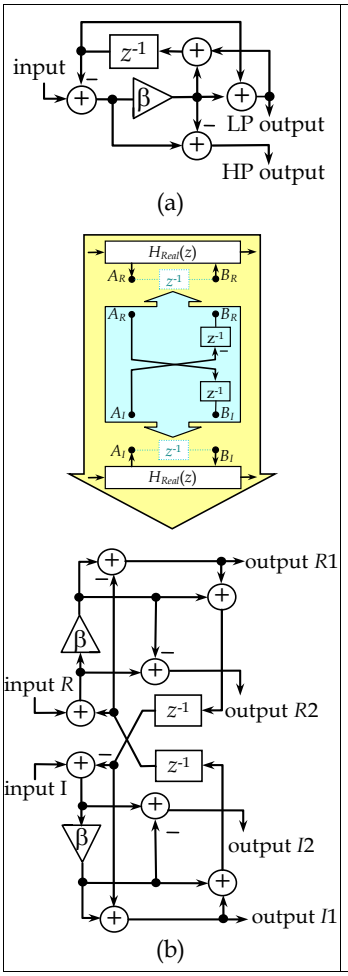


$$H(z)_{LS1b}^{LP} = \beta\frac{1+z^{-1}}{1-(1-2\beta)z^{-1}} \tag{18}$$

$$H(z)_{LS1b}^{HP} = (1-\beta)\frac{1-z^{-1}}{1-(1-2\beta)z^{-1}} \tag{19}$$

$$z^{-1} \rightarrow -jz^{-1}$$

$$H_{LS1b-LP}^{RR1}(z) = H_{LS1b-LP}^{II1}(z) = H_{LS1b-LP}^{R} = \beta\frac{1+(2\beta-1)z^{-2}}{1+(2\beta-1)^2 z^{-2}}; \tag{20}$$

$$H_{LS1b-LP}^{RI1}(z) = -H_{LS1b-LP}^{IR1}(z) = H_{LS1b-LP}^{I} = \frac{\beta(1-\beta)2z^{-1}}{1+(2\beta-1)^2 z^{-2}}; \tag{21}$$

$$H_{LS1b-HP}^{RR2}(z) = H_{LS1b-HP}^{II2}(z) = H_{LS1b-HP}^{R} = (1-\beta)\frac{1+(1-2\beta)z^{-2}}{1+(2\beta-1)^2 z^{-2}}; \tag{22}$$

$$H_{LS1b-HP}^{RI2}(z) = -H_{LS1b-HP}^{IR2}(z) = H_{LS1b-HP}^{I} = \frac{-2z^{-1}\beta(1-\beta)}{1+(2\beta-1)^2 z^{-2}}; \tag{23}$$

Fig. 6. LS1b orthogonal complex section derivation (Watanabe-Nishihara transformation).

The same approach, when applied to the MHNS real filter-prototype section, produces the orthogonal complex MHNS structure (Stoyanov et al., 1996).

Fig. 7a depicts the worst-case gain-sensitivities for the same pole positions in LS1b and MHNS universal real filter-prototypes. It is apparent that the LS1b real section shows around a hundred times lower sensitivity than the MHNS real structure in almost the entire frequency range – from 0 to $\omega_s/2$. The LS1b-section realizes unity gain on both its outputs, it is canonic with respect to the multipliers and exhibits very low sensitivity in the important applications of narrowband LP and wideband HP filters.

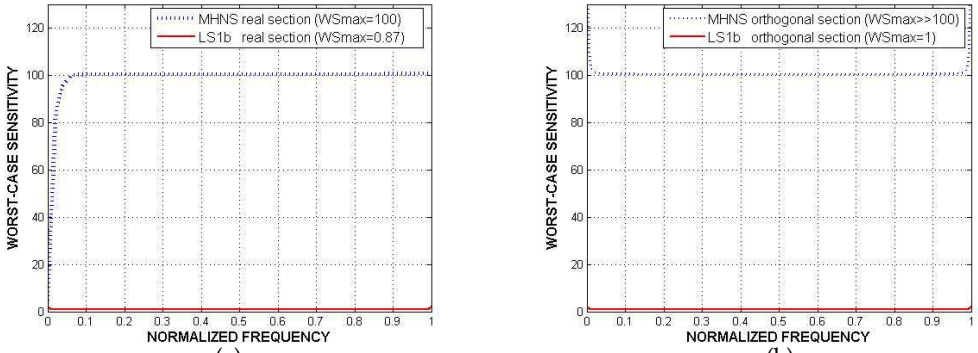


(a) (b)

Fig. 7. Worst-case sensitivities for the LS1b and MHNS filters (a) real –prototypes (LP outputs); (b) orthogonal structures for real input – real output BP transfer functions.

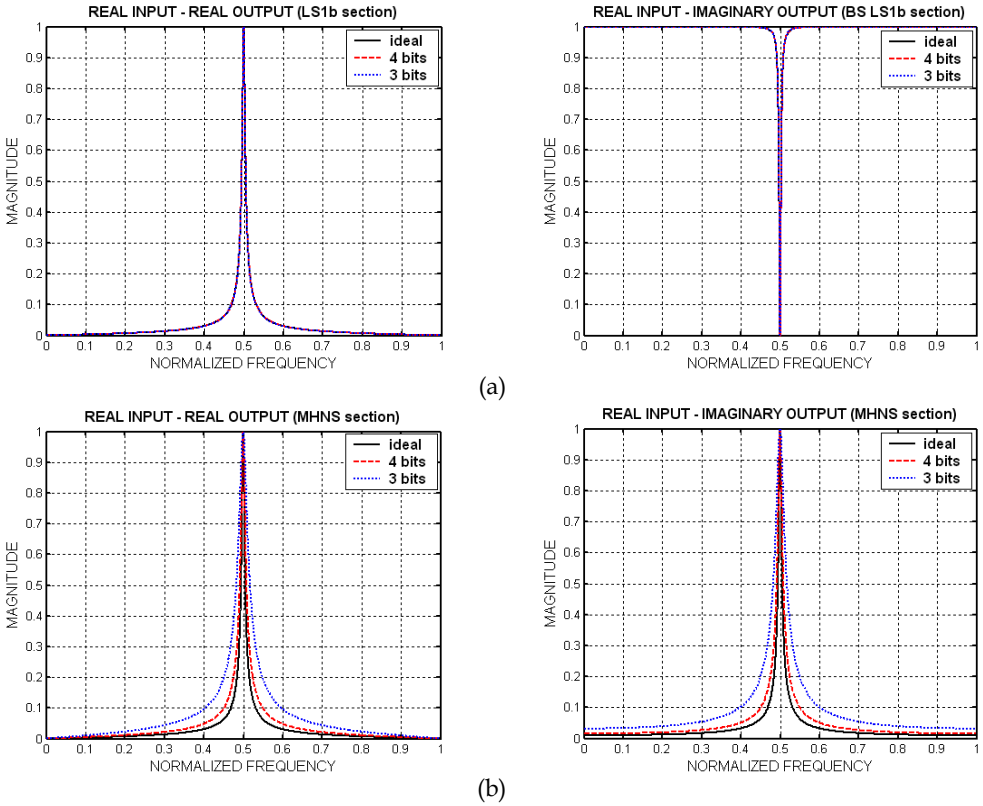


(a)

(b)

Fig. 8. Magnitude responses of the LS1b (a) and MHNS (b) orthogonal complex filter sections for different word-lengths.

For the same poles ($\alpha$=0.99 and $\beta$=0.005), the worst-case sensitivity is also investigated for the orthogonal complex structures. In Fig. 7b graphical results for the BP transfer functions $H^{R}_{LS1b-LP}(z)$ and $H^{R}_{MHNS-LP}(z)$ are presented. The sensitivity of the LP LS1b-based orthogonal section is approximately a hundred times lower over the whole frequency range. Hence, in terms of sensitivity, the orthogonal structures have the same behaviour pattern as their real filter-prototypes.
Some experimental results of the magnitude responses following the quantization of $\alpha$ and $\beta$ multipliers are shown in Fig. 8. Canonic Sign-Digit Code (CSDC) is used, together with fixed point arithmetic. Narrowband BP and BS orthogonal complex filters are investigated for poles close to the unit circle ($p_{1,2}=\pm j0.99$). The magnitude response of the LS1b orthogonal complex filter does not deteriorate but coincides with the ideal when the word-length is 4, or even 3, bits (Fig. 8a). The MHNS orthogonal structure (Fig. 8b) is more sensitive, and its magnitude response changes significantly, for both 3-bit and 4-bit word-lengths. The pass-band expands while the attenuation in the stop-bands decreases. Hence, the low-sensitivity structure LS1b is a better choice for applications involving analytic signal processing.

### 2.3. Low-Sensitivity Orthogonal Complex Second-Order IIR Filter Sections

In the odd-order cascade filter structures there is one first-order section, the rest being second-order. These sections may have higher sensitivity than the first-order sections and can be more seriously affected by parasitic effects - the limit cycles and quantization noises can completely disrupt the filtering process. This is why the second-order filter sections are better investigated and a large number of sections already exists.
A very low-sensitivity second-order orthogonal complex filter section, named LS2, is derived and comparatively investigated (Stoyanov et. al., 1997), (Stoyanov et al., 1996). This structure, obtained after the Watanabe-Nishihara circuit transformation is applied to the LS2 real filter-prototype (Fig. 9a), is shown in Fig. 9b. All the transfer functions of the LS2 orthogonal section are of BP type except for (28), which are BS.
The orthogonal complex LS2 filter section is compared with two other often-studied second-order orthogonal complex sections: DF-section (Direct Form) (Eswaran et al., 1991) and MN-section (Minimum Norm) (Nie et al., 1993). Both real filter-prototypes and orthogonal complex filters are investigated, when realizing the same poles of the transfer function, in (Stoyanov et. al., 1997), (Stoyanov et al., 1996).
In Fig. 10a the worst-case gain-sensitivities for the real prototypes are depicted. The results convincingly show that the sensitivity of the LS2 real filter section is thousands of times lower than the sensitivity of the other two real sections. The LS2 section is canonic with respect to the multipliers but a higher number of adders is the price for its very low sensitivity.
In Fig. 10b the worst-case gain-sensitivities of the BP transfer functions when real input and real output are used for the three orthogonal structures are shown. It is clearly seen that the LS2 orthogonal section has a tenfold lower sensitivity compared to the MN and DF orthogonal structures, while using more than three times fewer multipliers. The same results were also obtained for the other transfer functions (Stoyanov et. al., 1997).

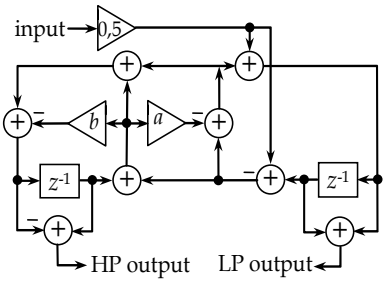


(a)

$$H_{LS2}^{LP}(z)=0{,}5a\frac{1+2z^{-1}+z^{-2}}{1+(-2+b+2a)z^{-1}+(1-b)z^{-2}} \quad (24)$$

$$H_{LS2}^{HP}(z)=0{,}5\frac{(2-a-b)(1-2z^{-1}+z^{-2})}{1+(-2+b+2a)z^{-1}+(1-b)z^{-2}} \quad (25)$$

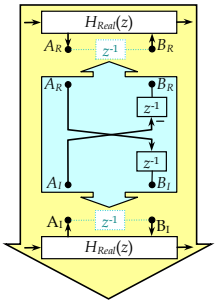


$$z^{-1}\rightarrow -jz^{-1}$$

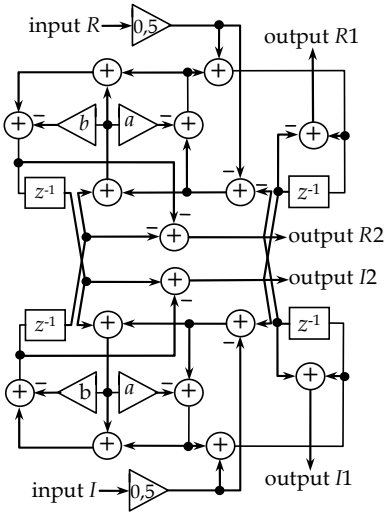


(b)

$$H_{LS2-LP}^{RR1}(z)=H_{LS2-LP}^{II1}(z)=H_{LS2-LP}^{R}(z)= =0{,}5a\frac{1+(4a+3b-6)z^{-2}+(1-b)z^{-4}}{1+\left[(2a+b-2)^2-2(1-b)\right]z^{-2}+(1-b)^2z^{-4}} \quad (26)$$

$$H_{LS2-LP}^{RI1}(z)=-H_{LS2-LP}^{RI1}(z)=H_{LS2-LP}^{I}(z)= =0{,}5\frac{az^{-1}\left[(4-2a-b)+(2a+3b-4)z^{-2}\right]}{1+\left[(2a+b-2)^2-2(1-b)\right]z^{-2}+(1-b)^2z^{-4}} \quad (27)$$

$$H_{LS2-HP}^{RR2}(z)=H_{LS2-HP}^{II2}(z)=H_{LS2-HP}^{R}(z)= =0{,}5\frac{(2-a-b)\left[1+(2-4a-b)z^{-2}+(1-b)z^{-4}\right]}{1+\left[(2a+b-2)^2-2(1-b)\right]z^{-2}+(1-b)^2z^{-4}} \quad (28)$$

$$H_{LS2-HP}^{RI2}(z)=-H_{LS2-HP}^{RI2}(z)=H_{LS2-HP}^{I}(z)= =0{,}5\frac{(2-a-b)\left[(-2a-b)+(2a-b)z^{-2}\right]z^{-1}}{1+\left[(2a+b-2)^2-2(1-b)\right]z^{-2}+(1-b)^2z^{-4}} \quad (29)$$

Fig. 9. Orthogonal complex LS2 second-order filter section derivation.

It is clear from Fig. 10a and 10b that the orthogonal structures inherit the sensitivity of their real filter-prototypes and that the shapes of the worst-case sensitivity curves are transferred from the prototypes to the orthogonal structures, becoming symmetric around the frequency $\omega_s/4$.

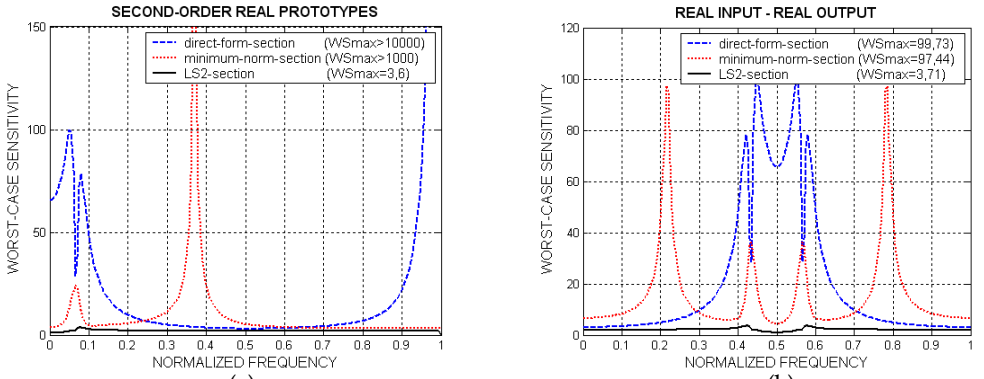


(a) (b)

Fig. 10. Worst-case sensitivities for the DF, MN and LS2 filters (a) real –prototypes (LP outputs); (b) orthogonal structures for real input – real output BP transfer functions.

The effect of the coefficient quantization on the magnitude responses is experimentally investigated and some of the results for the three orthogonal structures are shown in Fig. 11.

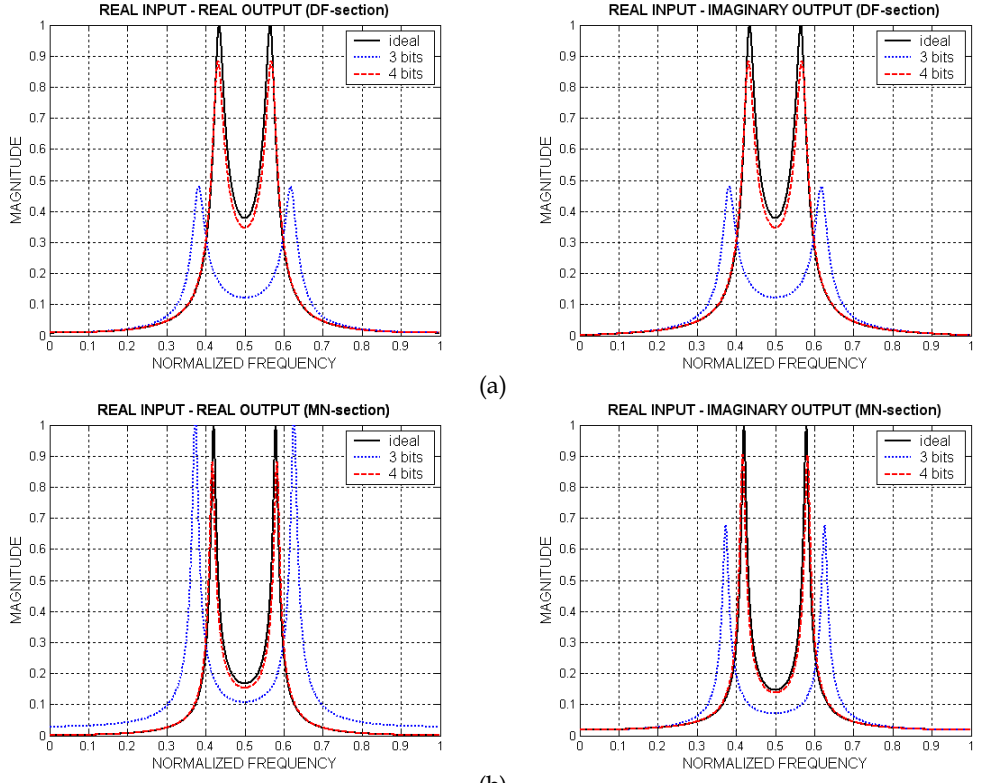


(a)

(b)

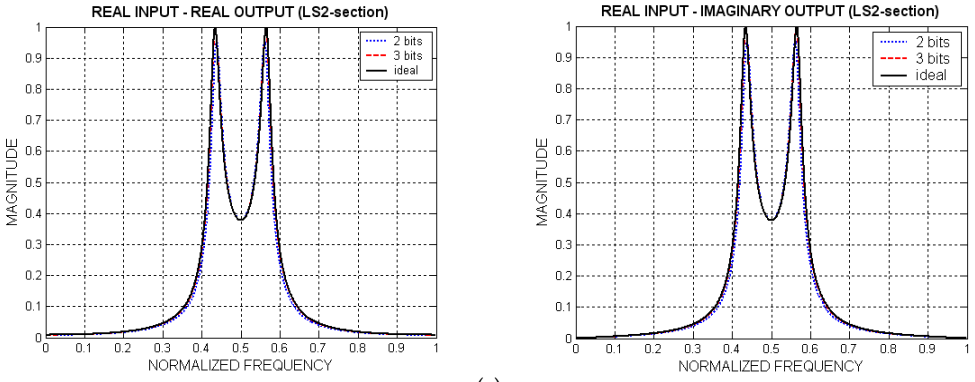


(c)

Fig. 11. Magnitude responses of the second-order orthogonal filter sections for different word-lengths (a) DF; (b) MN; (c) LS2.

It can be seen that the LS2 orthogonal structure has a magnitude response almost coinciding with the ideal one, even when the word-length is reduced to only 3 bits (Fig. 11c), whilst the DF-structure magnitude response is considerably changed when the word-length is 4 bits and deteriorates completely when the quantization is 3 bits (Fig. 11a). Similar behaviour is observed also in the MN-orthogonal filter section (Fig. 11b).

The low-sensitivity orthogonal complex first- and second-order sections presented in this section can be used as building blocks for a higher order cascade digital filter design. Their low sensitivities also ensure the low sensitivity of the cascade filter structure. Low sensitivity reduces the effect of the possible mismatch between the real and imaginary channels of the complex filter, which may have a crucial effect on the circuit performance.

Low-sensitivity orthogonal sections are very useful in analytic signal processing applications, permitting a considerable reduction in both the complexity and cost of the equipment.

## 3. Variable Complex IIR Digital Filters

### 3.1 Overview

Variable digital filters (VDF) with independently tunable central frequency $\omega_c$ and bandwidth (BW) are needed for many applications such as digital audio and video processing, medical electronics, radar systems, wireless communications etc. An overview of all the main approaches to the designed structures of FIR and IIR digital filters is set out in (Stoyanov & Kawamata, 1997).

Complex coefficient VDFs provide additional advantages in processing both real and complex signals, which are frequently encountered in telecommunications.

Real and complex VDFs are usually designed by employing the all-pass Constantinides transformations, consisting of the replacement of all delay elements in the LP filter-prototype with different all-pass sections. However, when the prototype is of IIR type it is difficult to avoid producing delay-free loops. The best-known method partly solving the problem is that of Mitra, Nevuvo and Roivainen (MNR-method) (Mitra et al., 1990-b), based on parallel all-pass real or complex structures and employing truncated Taylor series expansions of the filter coefficients to calculate them after the all-pass transformations. The

method is good for real digital filters but in the case of complex filters there are two series truncations and, as a result, a tuning of the BW without degradation of the magnitude characteristics is possible only over a very narrow frequency band. The other main disadvantage of the method is the high stop-band sensitivity, which causes additional degradation of the filter characteristics. There is yet another approach (Murakoshi et al., 1994), based on a circuit transformation proposed in (Watanabe & Nishihara, 1991), which is able to turn any real circuit into a complex one. Using some new transformations, variable complex BP/BS filters with tunable BW, but with one cut-off frequency remaining fixed, are obtained. The variable BP filter in (Murakoshi et al., 1994) employs too many elements and there are limitations in respect of the BW and requirements for fixing one of the pass-band edges.
This section examines a method of designing complex variable filters with independently tunable central frequency and BW, which has a wider range of tuning of the BW and lower stop-band sensitivity than those in (Mitra et al., 1990-b) and reduced complexity and higher freedom of tuning compared to those in (Murakoshi et al., 1994).

### 3.2 Variable Complex Filter Design Procedure Outline

For any given specifications or more general requirements for the desired complex BP or BS filter, the design procedure consists of the following steps (Stoyanov & Nikolova, 1999):

1. Shift the given BP or BS arithmetically symmetric magnitude specifications along the frequency axes until the zero frequency coincides with the central frequency $\omega_c$ of the specifications, thus turning them into LP or HP type.

2. Apply any possible approximation - classical or more general. As a result an LP or HP real coefficient transfer function is obtained.

3. Factor the transfer function to second-order (and possibly one first-order) terms and design the corresponding LP/HP first and second-order filter sections. For each section apply the Constantinides LP to LP spectral transformation:

$$z^{-1} \to \frac{z^{-1} - \beta}{1 - \beta z^{-1}} = T(z)\,. \tag{30}$$

This produces a composite multiplier coefficient $\hat{\beta}$ that is a function of $\beta$ and makes the BW variable.

4. Expand the composite multipliers $\hat{\beta}$ into Taylor series and take only the linear terms, thereby ensuring that the BW variable real LP / HP digital filters will not contain delay-free loops.

5. Using complex transformation (2) $z^{-1} \to z^{-1}e^{j\theta} = z^{-1}\left(\cos\theta + j\sin\theta\right)$ or the circuit transformation (Watanabe & Nishihara, 1991) applied to the designed real filter sections, obtain the complex coefficient structures with variable central frequency $\omega_c$ changed independently of $\theta$.

The proposed design procedure produces no delay-free loops, even if only one Taylor series truncation is used. The method permits the design of BP/BS filters of any even order and any possible approximation can be applied. It is also free from BW limitations and from the requirement to fix some of the pass-band edge frequencies encountered in some other design methods.

### 3.3 High Tuning Accuracy Variable Complex Digital Filters Sections

The Constantinides LP to LP spectral transformation (30), applied on LS1b universal section's LP (18) and HP (19) real transfer functions, transforms them into BW-variable real transfer functions:

$$\hat{H}(z)_{LS1b}^{LP} = \hat{\beta}\frac{1+z^{-1}}{1-\left(1-2\hat{\beta}\right)z^{-1}}; \qquad \hat{H}(z)_{LS1b}^{HP} = \left(1-\hat{\beta}\right)\frac{1-z^{-1}}{1-\left(1-2\hat{\beta}\right)z^{-1}}. \tag{31}$$

The composite multiplier $\hat{\beta}$ (Fig. 12) is expanded into a Taylor series and only the linear terms are taken:

$$\hat{\beta} = \beta + \gamma c_1, \text{ where } c_1 = 2\beta(\beta-1). \tag{32}$$

The BW can be tuned to some extent by changing $\gamma$ ($\gamma$ <0 - wider BW; $\gamma$ >0 - narrower BW).

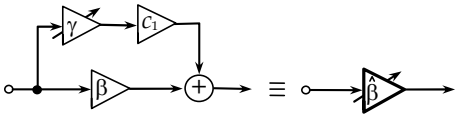


Fig. 12. Composite multiplier $\hat{\beta}$ tuning the BW.

The complex transformation (2) is applied on BW-variable real LP and HP transfer functions (31), thus obtaining the complex coefficient transfer functions, variable in regard to the central frequency $\omega_c$, tuned by changing $\theta$. For the variable complex LS1b digital filter structure (Fig. 13) the variable transfer functions are:

$$\hat{H}_{LS1b-LP}^{RR1}(z) = \hat{H}_{LS1b-LP}^{II1}(z) = \hat{\beta}\frac{1+2\hat{\beta}\cos\theta z^{-1}+\left(2\hat{\beta}-1\right)z^{-2}}{1+2\left(2\hat{\beta}-1\right)\cos\theta z^{-1}+\left(2\hat{\beta}-1\right)^2 z^{-2}}; \tag{33}$$

$$\hat{H}_{LS1b-LP}^{RI1}(z) = -\hat{H}_{LS1b-LP}^{IR1}(z) = \hat{\beta}\frac{2\left(1-\hat{\beta}\right)\sin\theta z^{-1}}{1+2\left(2\hat{\beta}-1\right)\cos\theta z^{-1}+\left(2\hat{\beta}-1\right)^2 z^{-2}}; \tag{34}$$

$$\hat{H}_{LS1b-HP}^{RR2}(z) = \hat{H}_{LS1b-HP}^{II2}(z) = \left(1-\hat{\beta}\right)\frac{1-2\left(1-\hat{\beta}\right)\cos\theta z^{-1}+\left(1-2\hat{\beta}\right)z^{-2}}{1+2\left(2\hat{\beta}-1\right)\cos\theta z^{-1}+\left(2\hat{\beta}-1\right)^2 z^{-2}}; \tag{35}$$

$$\hat{H}_{LS1b-HP}^{RI2}(z) = -\hat{H}_{LS1b-HP}^{IR2}(z) = \left(1-\hat{\beta}\right)\frac{-2\hat{\beta}\sin\theta z^{-1}}{1+2\left(2\hat{\beta}-1\right)\cos\theta z^{-1}+\left(2\hat{\beta}-1\right)^2 z^{-2}}. \tag{36}$$

All of these are of BP type except (35), which are of BS type. The variable complex LS1b digital filter performance is verified by extensive simulations. Fig. 14 shows how the central frequency $\omega_c$ of narrowband ($\beta$ = 0.98) variable complex BP (33) and BS (35) transfer functions are tuned by changing $\theta$. It is obvious that $\omega_C$ can be tuned without any limitations over the entire frequency range.

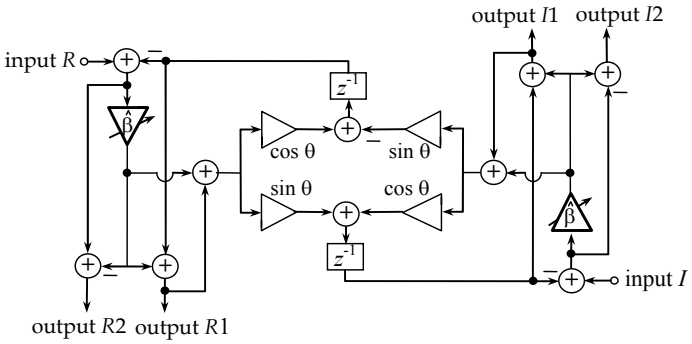


Fig. 13. Variable complex LS1b digital filter structure.

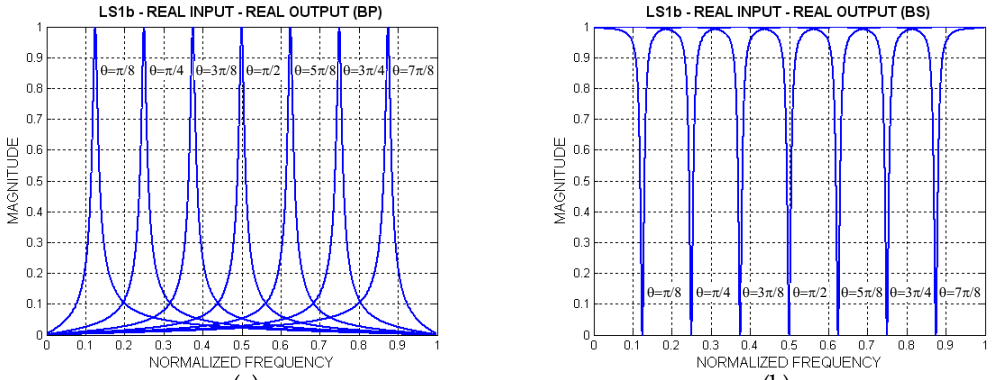


Fig. 14. Magnitude responses of variable BP (a) and BS (b) variable complex LS1b section for different values of θ and fixed γ=0.

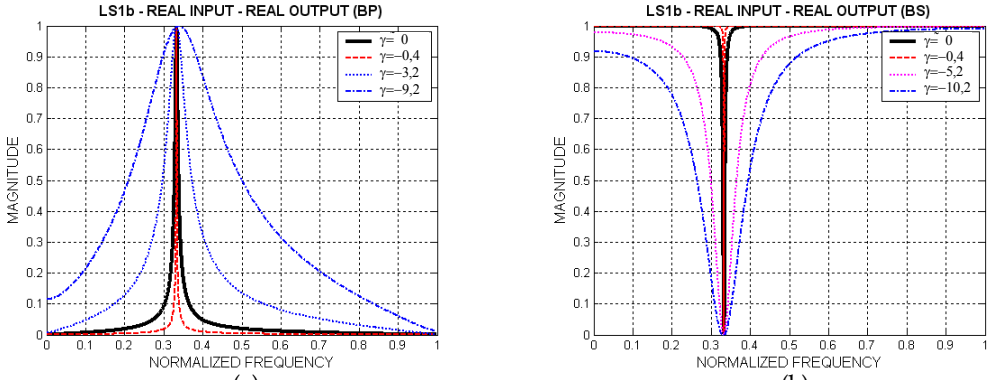


Fig. 15. Magnitude responses of variable BP (a) and BS (b) variable complex LS1b section for different values of γ and fixed θ=π/3.

In Fig. 15 the tuning of the BW of the same LS1b by changing γ is demonstrated.

In Fig. 16 the behaviour of the complex LS1b and MHNS variable digital filters in a limited wordlength is compared. It is clear that the characteristics of the MHNS-based complex filter are changed considerably after the multiplier coefficients' truncation to 4 or 3 bits while those of the LS1b-based complex filter remain practically unchanged. This is due to the very low sensitivity inherited from the LS1b prototype.

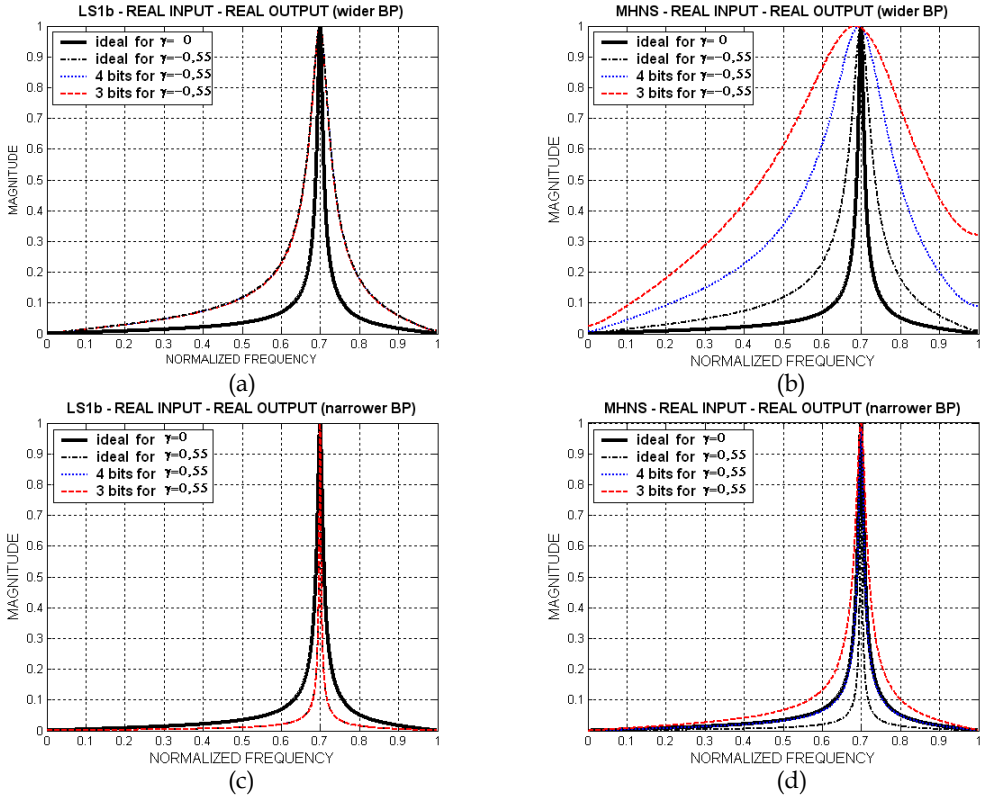


Fig. 16. Magnitude responses of the variable complex BP LS1b and MHNS for different coefficients word-length and BW tuned (θ=7π/10).

The improved design method proposed in this section is also applicable to real second-order filter sections – the LS2 (Fig. 9a) and DF (Eswaran et al., 1991). The variable complex LS2 structure is shown in Fig. 17 and the transfer functions that it realizes are:

$$\hat{H}^{RR1}_{LS2-HЧ}(z)=\hat{H}^{II1}_{LS2-HЧ}(z)= =\frac{\hat{a}}{2}\frac{1+\left[\left(2\hat{a}+\hat{b}\right)A\right]z^{-1}+\left[2\left(2\hat{a}+\hat{b}-2\right)+\left(2-\hat{b}\right)\left(A^2-C^2\right)\right]z^{-2}+\left[\left(2\hat{a}-\hat{b}\right)A\right]z^{-3}+\left(1-\hat{b}\right)z^{-4}}{D(z)} \quad (37)$$

$$\hat{H}^{RI1}_{LS2-BЧ}(z) = -\hat{H}^{IR1}_{LS2-BЧ}(z) = \frac{\hat{a}}{2}\frac{\left(4-2\hat{a}-\hat{b}\right)Cz^{-1} + 2\hat{b}ACz^{-2} + \left(2\hat{a}+3\hat{b}-4\right)Cz^{-3}}{D(z)} \tag{38}$$

$$\hat{H}^{RR2}_{LS2-BЧ}(z) = \hat{H}^{II2}_{LS2-BЧ}(z) = \\ = B\frac{1+\left[\left(2\hat{a}+\hat{b}-4\right)A\right]z^{-1} + \left[-2\left(2\hat{a}+\hat{b}-2\right)+\left(2-\hat{b}\right)\left(A^2-C^2\right)\right]z^{-2} + \left[\left(2\hat{a}+3\hat{b}-4\right)A\right]z^{-3} + \left(1-\hat{b}\right)z^{-4}}{D(z)} \tag{39}$$

$$\hat{H}^{RI2}_{LS2-BЧ}(z) = -\hat{H}^{IR2}_{LS2-BЧ}(z) = B\frac{\left(-2\hat{a}-\hat{b}\right)Cz^{-1} + 2\hat{b}ACz^{-2} + \left(2\hat{a}-\hat{b}\right)Cz^{-3}}{D(z)} \tag{40}$$

where $A$=cos θ, $C$=sin θ, $B = 0{,}5\left(2-\hat{a}-\hat{b}\right)$, and

$$D(z) = 1 + 2\left(2\hat{a}+\hat{b}-2\right)Az^{-1} + \left[\left(2\hat{a}+\hat{b}-2\right)^2 + 2\left(1-\hat{b}\right)\left(A^2-C^2\right)\right]z^{-2} + 2\left(1-\hat{b}\right)\left(2\hat{a}+\hat{b}-2\right)Az^{-3} + \left(1-\hat{b}\right)^2 z^{-4}.$$

Composite multipliers $\hat{a}$ and $\hat{b}$ have analytical expressions, analogous to (32). The coefficient θ changes the central frequency $\omega_c$, while the BW is changed by γ (the composite multipliers $\hat{a}$ and $\hat{b}$ are functions of γ).

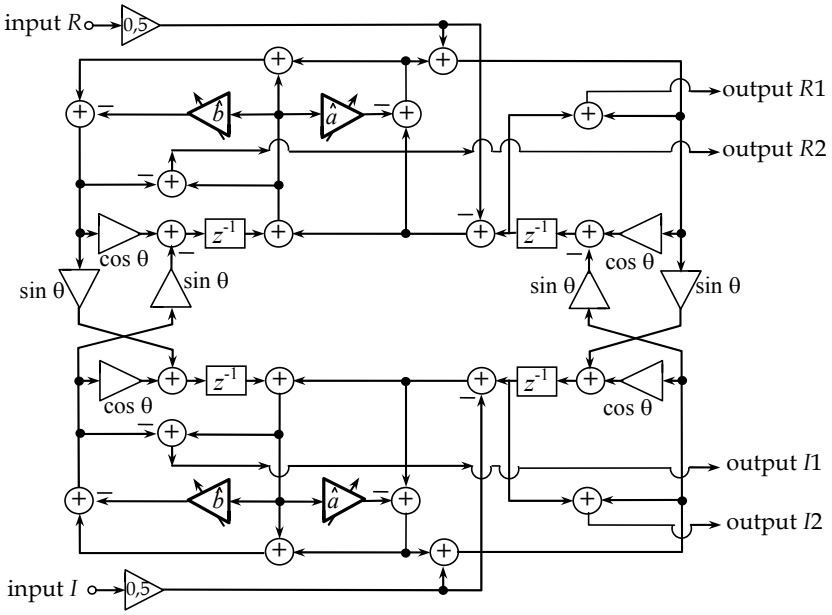


Fig. 17. Variable complex second-order LS2 digital filter section.

Fig. 18 and Fig. 19 show experimental results in regard to the tuning abilities of the BP (37) and BS (39) transfer functions.

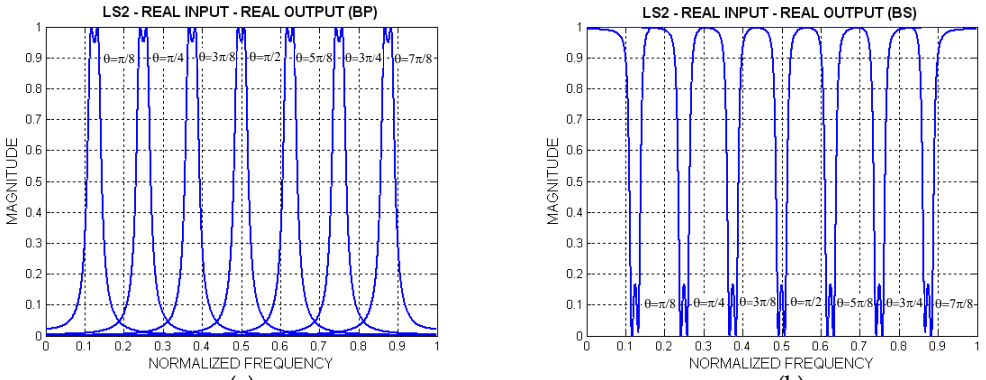


(a) (b)

Fig. 18. Magnitude responses of variable BP (a) and BS (b) complex LS2 section for different values of θ (central frequency tuning) and fixed γ=0.

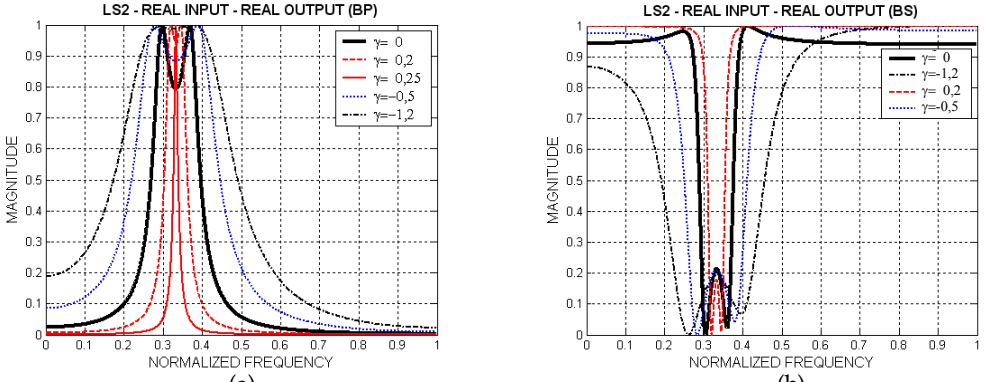


(a) (b)

Fig. 19. Magnitude responses of variable BP (a) and BS (b) complex LS2 section for different values of γ (BW tuning) and fixed θ=π/3.

Variable complex LS2 and DF digital filter structures are compared for different word-lengths of the coefficients and the experimental results are depicted in Fig. 20.

The graphics in Fig. 20 show that the low-sensitivity LS2 variable complex section is undoubtedly superior to the DF section when the coefficients are quantized.

The variable complex DF filter does not preserve the magnitude shape either when the BW is made wider or when it is narrower. In addition, the DF-attenuation in the pass-band increases two-fold for a word-length of 3 bits (Fig. 20b,d) whilst in the LS2 structure it remains unchanged throughout the whole frequency range.

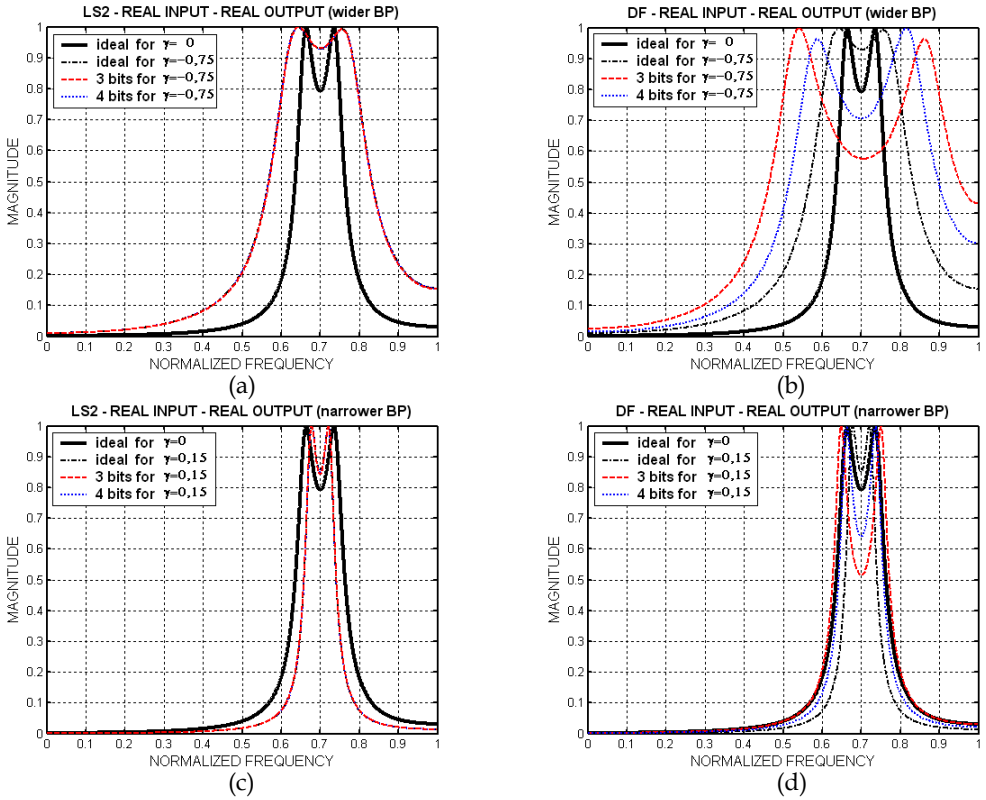


Fig. 20. Magnitude responses of the variable complex BP LS2 and DF for different coefficients word-length and BW tuned ($\theta=7\pi/10$).

### 3.4 Design Example and Experiments

To demonstrate the advantages of the proposed improved method for designing variable complex filters, a design example will be displayed (Stoyanov & Nikolova, 1999). Two eighth-order variable complex filters will be compared to each other – an LS2-based cascade structure and an MNR-method-based all-pass structure (Mitra et. al., 1990-b).

The required specification is as follows: a variable complex BP filter with pass-band tuned from 0.04 to 0.16 (nominal value 0.1), intermediate band 0.06, $R_p = 2$ dB, $R_s = 40$ dB and central frequency $\omega_c$ tuned over the entire frequency range $0 \div 1$. Following the procedure given in section 3.2, and using a Chebyshev approximation, a fourth-order LP transfer function is obtained. It is presented as a cascade realization consisting of two second-order terms. Worst-case sensitivities of the LP second-order LS2-based and parallel all-pass structure are examined and the results are depicted in Fig. 21. It is obvious that the LS2-section has about 50 times lower sensitivity in the pass-band than the all-pass structure. On the other hand, in the stop-band the parallel all-pass structure shows lower sensitivity.

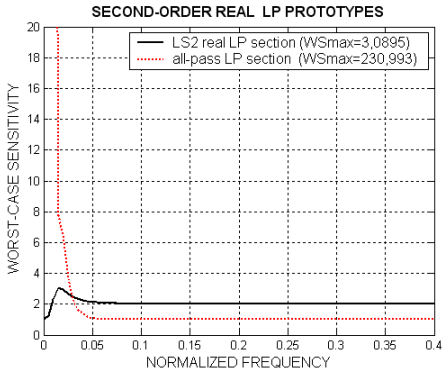


Fig. 21. Worst-case sensitivity of second-order LS2 and all-pass real digital filter sections.

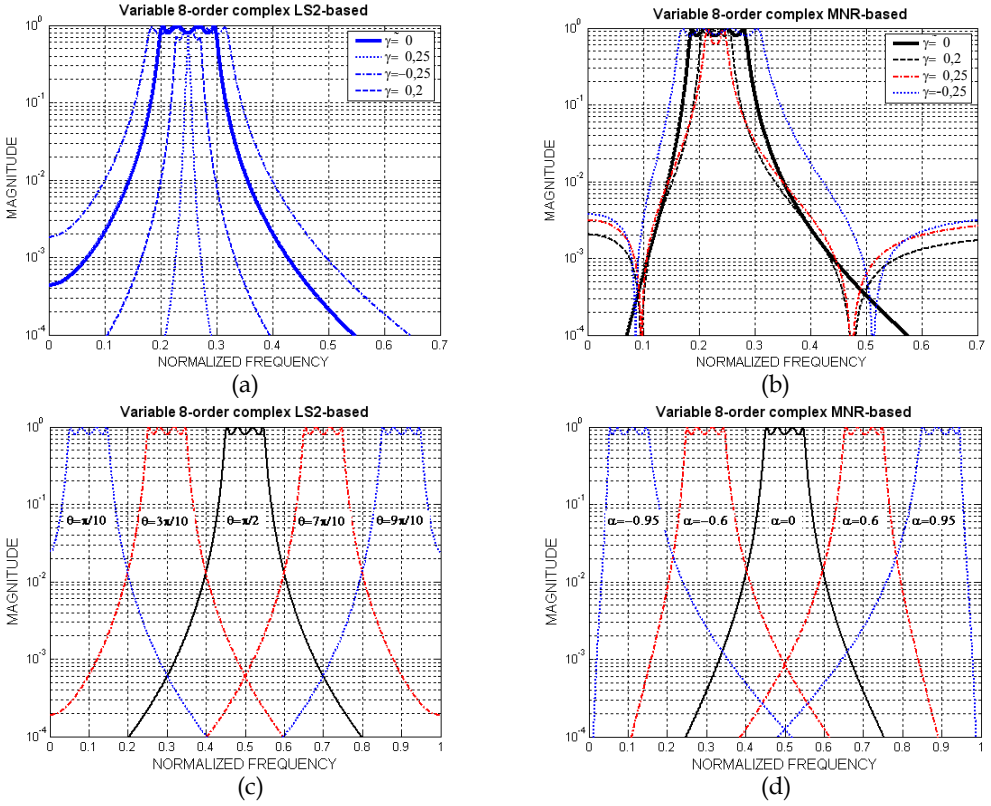


Fig. 22. Magnitude responses of the variable complex BP eighth-order LS2-based and MNR-based filters – BW tuning (a,b – for $\theta=\pi/4$) and central frequency tuning (c,d – for $\gamma=0$).

Then, a variable complex filter using two sections identical to the one in Fig. 17 is designed and the eighth-order BP filter thus obtained is simulated. The results for the BW tuning are

shown in Fig. 22a, while those for central frequency tuning are in Fig. 22c. Next, a complex all-pass sections based variable filter, following the MNR-method, was designed and the results from the simulation for the BW and central frequency tuning are shown in Fig. 22b and Fig. 22d respectively. It can be seen that, while the BW of the LS2 filter is tuned without problem over a frequency range much wider than required, the MNR filter turns from a Chebyshev into a kind of elliptic when tuned. The possibilities of tuning in a narrowing direction are very limited (tuning after $\gamma>0.2$ is actually impossible) and the shape of the magnitude varies strongly during the tuning process. As far as the central frequency tuning is concerned, no problems were observed for either filter - as is apparent from Fig. 22c, d.
The behaviour of both filters in a limited word-length environment is also investigated and some results are shown in Fig. 23.

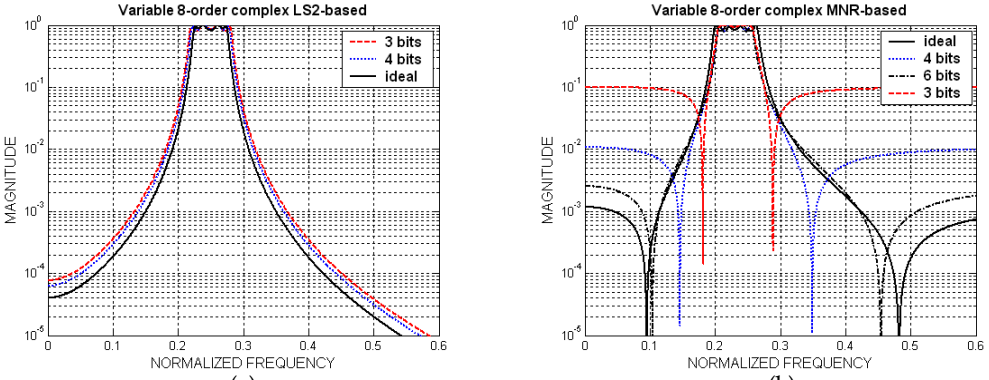


(a) (b)

Fig. 23. Magnitude responses of the variable complex BP eighth-order LS2-based (a) and MNR-based (b) filters for different coefficients word-length ($\gamma=0.15$; $\theta=\pi/4$).

While the LS2-based filter behaves well with 3-bits word-length, the magnitude response of the MNR-filter is strongly degraded even with 6-bit words, due to the higher sensitivity of the LP-prototype (Fig. 21) and the double usage of Taylor series truncation. Despite the lower sensitivity of the real all-pass structure in the stop-band (Fig. 21), the magnitude response of the obtained MNR-variable complex filter is completely degraded even for stop-band frequencies (Fig. 23b and Fig. 23b). The explanation lies in the imperfection of the MNR-method with respect to the variable complex filter design.
The complex coefficient variable BP and BS filters designed using the improved method examined in this section have a BW and central frequency which can be independently tuned with high accuracy. The possible BW tuning range is wider compared to that of the other known methods. The filter sections used have lower sensitivity and thus are less susceptible to the inaccuracies due to series truncations. The accuracy of tuning is higher and it is possible to use coefficients with a shorter word-length, thereby decreasing the power consumption and the volume of computations for both the filtering and updating of the coefficients. Similar results are obtained for other efficient IIR digital filter structures based on sensitivity minimization design, such as efficient multiplierless realizations and fractional-delay filters (Stoyanov et al., 2007).

## 4. Adaptive Complex Systems

### 4.1 Outline and Applications

FIR digital filter structures are usually preferred as the building blocks in adaptive systems, including complex ones, due to their absolute stability; however the use of IIR filters is increasing, owing to their definite advantages. A number of IIR adaptive complex filters were put forward as possible solutions to the problems typically encountered in many telecommunications applications dealing with the detection, tracking and suppression / elimination of complex signals embedded in noise. Wideband wireless communication systems are very sensitive to narrowband interference (NBI), which can even prevent the system operating (Giorgetti et al., 2005). For NBI suppression in quadrature phase shift keying (QPSK) spread-spectrum communication systems, an adaptive complex notch filter is used (Jiang et al., 2002).

Discrete multi-tone (DMT) modulation systems, such as DMT VDSL, are very sensitive to radio-frequency interference (RFI) and RFI-suppression has been discussed in many works, such as (Starr et al., 2003) (Yaohui et al., 2001). OFDM is the other leading technology for many broadband communication systems, such as MB-OFDM ultra wideband systems (UWB). As a result of NBI, signal-to-interference ratio (SIR) dropping can seriously degrade the characteristics of these systems (Carlemalm et al., 2004).

The problem of interference is encountered in various kinds of broadband telecommunications systems but the methods for interference suppression proposed so far can be broadly categorized into two approaches. The first concerns various frequency excision methods, whilst the second relates to so-called cancellation techniques. These techniques aim to eliminate or reduce interference in the received signal by the use of adaptive notch filtering-based methods or NBI identification (Baccareli et al., 2002).

This section deals with adaptive complex filtering as a noise-cancellation method associated with analytic signals and complex NBI suppression. An adaptive complex system is developed, based on the very low-sensitivity variable complex filters studied in section 3. The quality of adaptive filtering is influenced by two major factors – the efficiency and convergence of the adaptive algorithm, and the properties of the adaptive structure. Most research studies barely consider the details of adaptive filter realizations and their properties, although a lot has been done to improve the adaptive algorithms. The efficiency of adaptive complex filter sections and their beneficial properties considerably influence the adaptive process.

### 4.2 Adaptive Complex Systems Design

In Fig. 24 a block-diagram of an adaptive complex system is shown (Iliev et al., 2004).

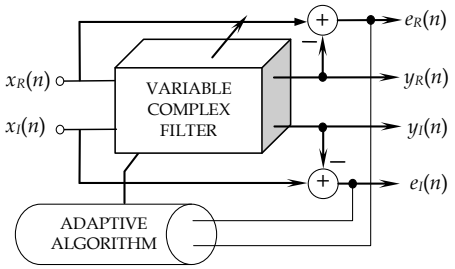


Fig. 24. Block-diagram of a BP/BS adaptive complex filter section.

The adaptive complex system design starts with a description of input-output equations. The BP/BS variable complex LS1b-based filter is considered and its BP real output is as follows:

$$y_R(n) = y_{R1}(n) + y_{R2}(n)\,, \tag{41}$$

where

$$\begin{aligned} y_{R1}(n) = &-2(2\beta-1)\cos\theta(n)y_{R1}(n-1) - (2\beta-1)^2 y_{R1}(n-2) + \\ &+ 2\beta x_R(n) + 4\beta^2\cos\theta(n)x_R(n-1) + 2\beta(2\beta-1)x_R(n-2) \end{aligned}; \tag{42}$$

$$\begin{aligned} y_{R2}(n) = &-2(2\beta-1)\cos\theta(n)y_{R2}(n-1) - (2\beta-1)^2 y_{R2}(n-2) - \\ &- 4\beta(1-\beta)\sin\theta(n)x_I(n-1). \end{aligned} \tag{43}$$

The imaginary output is given by the following equation:

$$y_I(n) = y_{I1}(n) + y_{I2}(n)\,, \tag{44}$$

where

$$\begin{aligned} y_{I1}(n) = &-2(2\beta-1)\cos\theta(n)y_{I1}(n-1) - (2\beta-1)^2 y_{I1}(n-2) + \\ &+ 4\beta(1-\beta)\sin\theta(n)x_R(n-1) \end{aligned}; \tag{45}$$

$$\begin{aligned} y_{I2}(n) = &-2(2\beta-1)\cos\theta(n)y_{I2}(n-1) - (2\beta-1)^2 y_{I2}(n-2) + \\ &+ 2\beta x_I(n) + 4\beta^2\cos\theta(n)x_I(n-1) + 2\beta(2\beta-1)x_I(n-2). \end{aligned} \tag{46}$$

For the BS variable complex LS1b filter there is a real output:

$$e_R(n) = x_R(n) - y_R(n)\,, \tag{47}$$

and an imaginary output:

$$e_I(n) = x_I(n) - y_I(n)\,. \tag{48}$$

The cost-function is the power of BS filter output signal:

$$[e(n)\,e^*(n)]\,, \tag{49}$$

where

$$e(n) = e_R(n) + je_I(n)\,. \tag{50}$$

At this stage an adaptive algorithm should be applied and the Least Mean Squares (LMS) algorithm is chosen since it combines low computational complexity and relatively fast adaptation rate. The LMS algorithm updates the filter coefficient responsible for the central frequency as follows:

$$\theta(n+1) = \theta(n) + \mu\,\mathrm{Re}[e(n)y'^*(n)]\,, \tag{51}$$

where μ is the step-size controlling the speed of convergence, (*) denotes complex-conjugate, $y'(n)$ is a derivative of $y(n) = y_R(n) + jy_I(n)$ with respect to the coefficient that is the subject of adaptation:

$$\begin{aligned} y_R'(n) = {} & 2(2\beta-1)\sin\theta(n)y_{R1}(n-1) - 4\beta^2\sin\theta(n)x_R(n-1) + \\ & + 2(2\beta-1)\sin\theta(n)y_{R2}(n-1) - 4\beta(1-\beta)\cos\theta(n)x_I(n-1) \end{aligned} \tag{52}$$

and

$$\begin{aligned} y_I'(n) = {} & 2(2\beta-1)\sin\theta(n)y_{I1}(n-1) + 4\beta(1-\beta)\cos\theta(n)x_R(n-1) + \\ & + 2(2\beta-1)\sin\theta(n)y_{I2}(n-1) - 4\beta^2\sin\theta(n)x_I(n-1). \end{aligned} \tag{53}$$

The adaptive process for the BP/BS variable complex second-order LS2-based filter can be similarly defined (Iliev et al., 2006).
In order to ensure the stability of the adaptive algorithm, the range of the step size μ should be set according to (Douglas, 1999):

$$0 < \mu < \frac{P}{N\sigma^2}. \tag{54}$$

In this case $N$ is the filter order, $\sigma^2$ is the power of the signal $y'(n)$ and $P$ is a constant which depends on the statistical characteristics of the input signal. In most practical situations $P$ is approximately equal to 0.1.

### 4.3 Adaptive Complex Filtering Investigations

The good performance of low-sensitivity complex filters in finite word-length environments and their low coefficient sensitivities significantly improve the quality of the adaptive filtering process and this will be experimentally confirmed. The narrowband low-sensitivity adaptive complex filters are examined for elimination / enhancement of narrowband complex signals. By changing the transformation factor $\theta$, the central frequency $\omega_c$ of the complex filter can be tuned over the entire frequency range adaptively. The accuracy of tuning is very high and it is possible to use coefficients with shorter word-length, thus decreasing the power consumption for both the adaptive filtering and the updating of the coefficients. The convergence of the adaptive algorithm for the developed low-sensitivity variable complex filters is investigated experimentally and the efficiency of the adaptation is demonstrated.
The experiments are conducted in three basic set-ups. First, we test the convergence speed of the adaptive complex filter sections with respect to different values of step size μ. In Fig. 25 the learning curves of this adaptation are shown. The input signal is a mixture of white noise and complex (analytic) sinusoid with frequency $f$ = 0.25. It can be observed that as the step-size increases a higher speed of adaptation is achieved. It obvious that the adaptive complex filter based on LS2 reaches steady state in the case of μ=0.005 after about 100 iterations (Fig. 25b), which is considerably less than the number of iterations needed for the filter based on LS1b (approximately 2000, Fig. 25a).

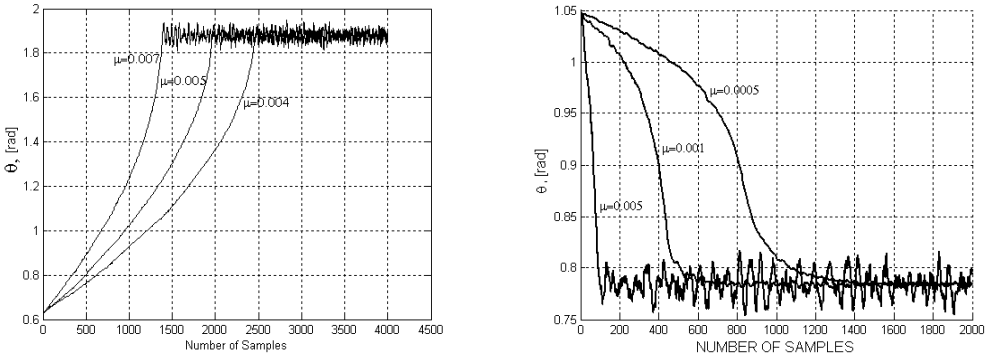


(a) (b)

Fig. 25. Trajectories of the coefficient θ for different step size μ for the (a) LS1b-based; (b) LS2-based complex filter section.

In Fig. 26 results for different filter BW are presented. It is clear that narrowing the filter BW slows the process of convergence. It should be mentioned that if some other (non low-sensitivity) adaptive complex sections were to be used, the coefficient β could not take values smaller than -0.1 without destroying the magnitude shape. Thus a faster convergence of the adaptive filtering can be obtained because of the wider BW. Comparing LS1b and LS2 realizations it can be concluded that, for the same BW, the LS2 filter converges 5 times faster.

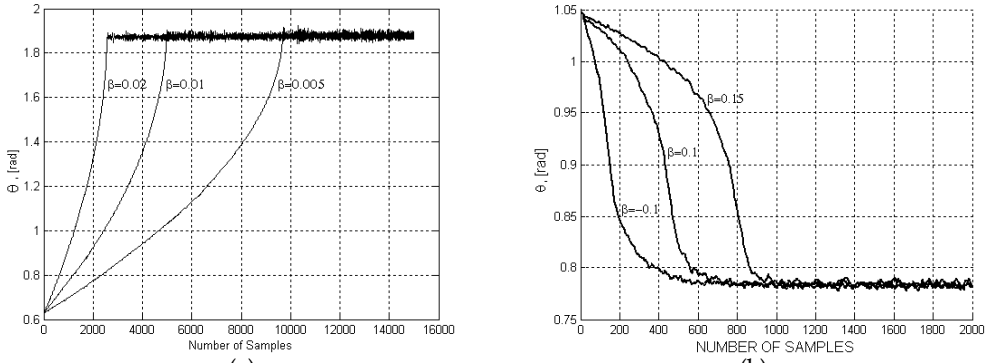


(a) (b)

Fig. 26. Trajectories of the coefficient θ for different BW β for the (a) LS1b-based; (b) LS2-based complex filter section.

Finally, Fig. 27 shows the behaviour of LS1b and LS2 filters for a wide range of frequencies. In all cases the low-sensitivity filter structures converge to the proper frequency value.

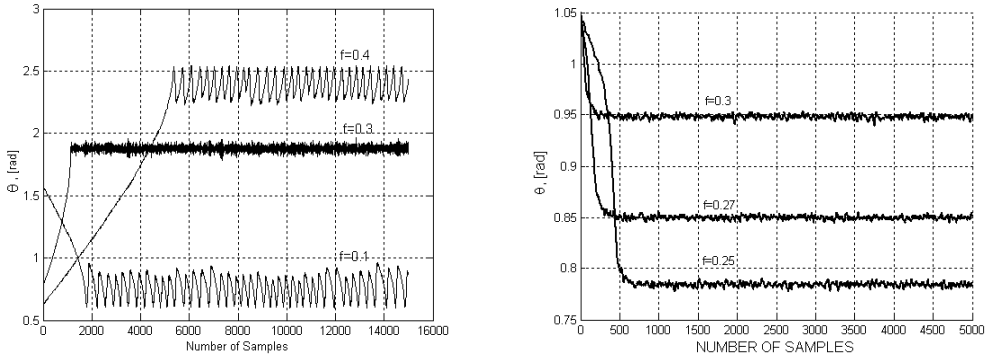


(a) (b)

Fig. 27. Trajectories of the coefficient θ for different frequency f for the (a) LS1b-based; (b) LS2-based complex filter section.

### 4.4 Adaptive Complex Filters Applications

The first- and second-order low-sensitivity adaptive complex filter sections examined in this section are suitable for both independent use and as building blocks for the higher order cascade or parallel realizations needed in many telecommunications applications.

Adaptive complex narrowband filtering is used for noise cancellation in an OFDM transmission scheme and shows that better SNR and bit-error rate (BER) performance can be achieved (Iliev et al., 2006). Another application of low-sensitivity narrowband adaptive complex filtering is NBI cancellation in MB-OFDM systems (Nikolova et al., 2006), multi-inputs multi-outputs (MIMO) OFDM systems (Iliev et al., 2009), and DMT VDSL systems (Ovtcharov et al., 2009-a). An advantage of the proposed scheme is that the adaptive complex system is universal, realizing BP and BS outputs simultaneously. Besides being suppressed, the NBI can also be monitored and the adaptive complex system can be deactivated when the interference disappears or is reduced to an acceptable level. In (Iliev et al., 2010) a method is proposed for NBI suppression in MIMO MB-OFDM UWB communication systems, using adaptive complex narrowband filtering based on the LS1b variable complex section. A comparative study shows that the NBI method is an optimal solution that offers a trade-off between outstanding NBI suppression efficiency and computational complexity. Various problems with OFDM systems and their possible solutions are summarized in (Nikolova et al., 2009); adaptive complex filtering is one of the most efficient methods for noise suppression in these systems (Nikolova et al., 2010). Adaptive complex filtering is an accurate and robust approach for RFI suppression in UWB communication systems (Ovtcharov et al., 2009-b) and GDSL MIMO systems (Poulkov et al., 2009).

## 5. Conclusions

Complex coefficient digital filters are used in many DSP applications relating to complex signal representations. Orthogonal signals occur often in different telecommunications applications and can be effectively processed by a special class of complex filters, the so-called orthogonal complex filters. A method for designing these filters is examined in this chapter and first- and second-order IIR orthogonal complex sections are synthesized. They

can be used as filter sections for designing cascade structures and also as single filter structures. The derived orthogonal sections are canonic very low-sensitivity structures which permit the use of a very short coefficient word-length, leading to higher accuracy, lower power consumption and simple implementation.
An improved method for designing variable complex filters is proposed. It is possible to use any classical or more general approximation, producing transfer function of any even order. The structures avoid delay-free loops and have a canonical number of elements. The variable complex filters designed with the improved method have central frequency and BW that are tuned independently and very accurately over a wide frequency range. Very narrowband BP/BS structures can be developed, such as the low-sensitivity LS1b and LS2 variable complex sections. Compared to other often-used methods they show higher freedom of tuning, reduced complexity and lower stop-band sensitivity.
A BP/BS adaptive complex system is developed based on the derived narrowband LS1b and LS2 variable complex filters, and the simple but efficient LMS adaptive algorithm. Both low-sensitivity adaptive complex sections are examined for suppression/enhancement of narrowband complex signals. They demonstrate excellent abilities and are appropriate to be applied in a number of telecommunications systems where the problem of eliminating complex noise, RFI or NBI exists.

## Acknowledgment

This work was supported by the Bulgarian National Science Fund – Grant No. ДО-02-135/2008 "Research on Cross Layer Optimization of Telecommunication Resource Allocation" and by the Technical University of Sofia (Bulgaria) Research Funding, Grant No. 102НИ065-07 "Computer System Development for Design, Investigation and Optimization of Selective Communication Circuits".

## 6. References

Baccareli, E.; Baggi, M. & Tagilione, L. (2002). A novel approach to in-band interference mitigation in ultra wide band radio systems. *IEEE Conf. on Ultra Wide Band Systems and Technologies*, pp. 297-301, 7 Aug. 2002.

Bello, P. A. (1963). Characterization of randomly time-variant linear channels, *IEEE Trans. on Commun. Syst.,* vol. CS-11, pp. 360-393, Dec. 1963.

Carlemalm, C.; Poor, H. V. & Logothetis, A. (2004). Suppression of multiple narrowband interferers in a spread-spectrum communication system. *IEEE Journal Select. Areas Commun.*, vol. 3, No.5, pp. 1431-1436, 2004.

Crystal, T. & Ehrman, L. (1968). The design and applications of digital filters with complex coefficients, *IEEE Trans. on Audio and Electroacoustics*, vol. 16, Issue: 3, pp. 315-320, Sept. 1968.

Douglas, S. (1999). Adaptive filtering, in *Digital signal processing handbook*, D. Williams & V. Madisetti, Eds., Boca Raton: CRC Press LLC, pp. 451-619, 1999.

Eswaran, C.; Manivannan, K. & Antoniou, A. (1991). An alternative sensitivity measure for designing low-sensitivity digital biquads, *IEEE Trans. on Circuits Syst.*, vol. CAS-38, No.2, pp. 218 - 221, Feb. 1991.

Giorgetti, A.; Chiani, M. & Win, M. Z. (2005). The effect of narrowband interference on wideband wireless communication systems. *IEEE Trans. on Commun.*, vol. 53, No. 12, pp. 2139-2149, 2005.

Helstrom, C. W. (1960). *Statistical theory of signal detection*, Pergamon, New York, 1960.

Iliev, G.; Nikolova, Z.; Poulkov, V. & Ovtcharov, M. (2010). Narrowband interference suppression for MIMO MB-OFDM UWB communication systems, *Intern. Journal on Advances in Telecommunications* (*IARIA Journals*), ISSN: 1942-2601, vol. 3, No. 1&2, pp. 1-8, 2010.

Iliev, G.; Nikolova, Z.; Poulkov, V. & Stoyanov, G. (2006). Noise cancellation in OFDM systems using adaptive complex narrowband IIR filtering, *IEEE Intern. Conf. on Communications (ICC-2006)*, Istanbul, Turkey, pp. 2859 – 2863, 11-15 June 2006.

Iliev, G.; Nikolova, Z.; Stoyanov, G. & Egiazarian, K. (2004). Efficient design of adaptive complex narrowband IIR filters, *Proc. of XII European Signal Proc. Conf. (EUSIPCO'04)*, pp. 1597-1600, Vienna, Austria, 6-10 Sept. 2004.

Iliev, G.; Ovtcharov, M.; Poulkov, V. & Nikolova, Z. (2009). Narrowband interference suppression for MIMO OFDM systems using adaptive filter banks, *The 5th Intern. Wireless Communications and Mobile Computing Conf. (IWCMC 2009) MIMO Systems Symp.*, pp. 874–877, Leipzig, Germany, 21-24 June 2009.

Jiang, H.; Nishimura, S. & Hinamoto, T. (2002). Steady-state analysis of complex adaptive IIR notch filter and its application to QPSK communication systems. *IEICE Trans. Fundamentals*, vol. E85-A, No. 5, pp. 1088-1095, May 2002.

Martin, K. (2003). Complex signal processing is not – complex, *Proc. of the 29th European Conf. on Solid-State Circuits (ESSCIRC'03)*, pp. 3-14, Estoril, Portugal, 16-18 Sept. 2003.

Martin, K. (2005). Approximation of complex IIR bandpass filters without arithmetic symmetry, *IEEE Trans. on Circuits Syst. I: Regular Papers*, vol. 52, No. 4, pp. 794 – 803, Apr. 2005.

Mitra, S. K.; Hirano, S.; Nishimura & Sugahara, K. (1990). Design of digital bandpass/ bandstop filters with independent tuning characteristics, *Frequenz*, vol. 44, No. 3-4, pp. 117- 121, 1990.

Mitra, S. K.; Neuvo, Y. & Roivainen, H. (1990). Design of recursive digital filters with variable characteristics, *Intern. Journal of Circuit Theory and Appl.*, vol. 18, No. 2, pp. 107-119, 1990.

Murakoshi, N.; Nishihara, A. & Watanabe, E. (1994). Synthesis of variable filters with complex coefficients, *Electronics and Commun. in Japan*, Part 3, vol. 77, No. 5, pp. 46-57, 1994.

Nie, H.; Raghuramireddy, D. & Unbehauen, R. (1993). Normalized minimum norm digital filter structure: a basic building block for processing real and complex sequences, *IEEE Trans. on Circuits Syst.-II: Analog and Digital Signal Proc.*, vol.40, No.7, pp. 449 - 451, July 1993.

Nikolova Z.; Iliev, G.; Ovtcharov, M. & Poulkov, V. (2009). Narrowband interference suppression in wireless OFDM systems, *African Journal of Information and Communication Technology,* vol. 5, No. 1, pp. 30-42, March 2009.

Nikolova, Z.; Poulkov, V.; Iliev, G. & Egiazarian, K. (2010). New adaptive complex IIR filters and their application in OFDM systems, *Journal of Signal, Image and Video Proc., Springer*, vol. 4, No. 2, pp. 197-207, June, 2010, ISSN: 1863-1703.

Nikolova, Z.; Poulkov, V.; Iliev, G. & Stoyanov, G. (2006). Narrowband interference cancellation in multiband OFDM systems, *3rd Cost 289 Workshop "Enabling Technologies for B3G Systems"*, pp. 45-49, Aveiro, Portugal, 12-13 July 2006.

Nishihara, A. (1980). Realization of low-sensitivity digital filters with minimal number of multipliers, *Proc. of 14th Asilomar Conf. on Cir., Syst. and Computers,* Pacific Globe, California, USA, pp. 219-223, Nov.1980.

Ovtcharov, M.; Poulkov, V.; Iliev, G. & Nikolova, Z. (2009), Radio frequency interference suppression in DMT VDSL systems, "*E+E*", ISSN:0861-4717, pp. 42 - 49, 9-10/2009.

Ovtcharov, M.; Poulkov, V.; Iliev, G. & Nikolova, Z. (2009). Narrowband interference suppression for IEEE UWB channels*, The Fourth Intern. Conf. on Digital Telecommunications (ICDT 2009),* pp. 43–47, Colmar, France, July 20-25, 2009.

Poulkov, V.; Ovtcharov, M.; Iliev, G. & Nikolova, Z. (2009). Radio frequency interference mitigation in GDSL MIMO systems by the use of an adaptive complex narrowband filter bank, *Intern. Conf. on Telecomm. in Modern Satellite, Cable and Broadcasting Services - TELSIKS-2009,* pp. 77 – 80, Nish, Serbia, 7-9 Oct. 2009.

Proakis, J. G. & Manolakis, D. K. (2006). *Digital signal processing*, Prentice Hall; 4th edition, ISBN-10: 0131873741.

Sim, P. K. (1987). SSB generation using complex digital filters, *IASTED Intern. Symp. on Signal Proc. and its Appl. (ISSPA'87)*, Brisbane, Australia, pp. 206 - 211, 24-28 Aug. 1987.

Starr, T.; Sorbara, M.; Cioffi, J. & Silverman, P. (2003). *DSL advances*, Prentice Hall, 2003.

Stoyanov, G. & Kawamata, M. (1997). Variable digital filters. *Journal of Signal Proc.*, vol. 1, No. 4, pp. 275- 290, July 1997.

Stoyanov, G.; Kawamata, M. & Valkova, Z. (1996) Very low-sensitivity complex coefficients bandpass filter sections, *Technical reports of IEICE. Sc. Meeting on Digital Signal Proc.*, Tokyo, Japan, vol. 96, No. 424, pp. 39-45, 13 Dec. 1996.

Stoyanov, G.; Kawamata, M. & Valkova, Z. (1997). New first and second-order very low-senitivity bandpass/bandstop complex digital filter sections, *Proc. IEEE Region 10th Annual Conf. "TENCON'97"*, Brisbane, Australia, vol.1, pp.61-64, 2-4 Dec. 1997.

Stoyanov, G. & Nikolova, Z. (1999). Improved method of design of complex coefficients variable IIR digital filters, *TELECOM'99*, Varna, Bulgaria, vol. 2, pp. 40-46, 26-28 Oct. 1999.

Stoyanov, G.; Nikolova, Z.; Ivanova, K. & Anzova, V. (2007). Design and realization of efficient IIR digital filter structures based on sensitivity minimizations, *Intern. Conf. on Telecomm. in Modern Satellite, Cable and Broadcasting Services - TELSIKS-2007,* vol.1, pp. 299 – 308, Nish, Serbia, 26 - 28 Sept. 2007.

Takahashi, A.; Nagai, N. & Miki, N. (1992). Complex digital filters with asymmetrical characteristics, *Proc. of IEEE Intern. Symp. on Circuits and Syst.* (*ISCAS'92*), vol. 5, pp. 2421 - 2424, San Diego, USA, June 1992.

Topalov, I. & Stoyanov, G. (1990). Low-sensitivity universal first-order digital filter sections without limit cycles, *Electronics Letters*, vol. 26, No.1, pp. 25-26, January 1990.

Watanabe, E. & Nishihara, A. (1991). A synthesis of a class of complex digital filters based on circuit transformation, *IEICE Trans. Fundamentals*, vol. E74, No.11, pp. 3622-3624, Nov. 1991.

Woodward, P. M. (1960). *Probability and information theory with application to radar,* Pergamon, New York, 1960.

Yaohui, L.; Laakso, T. I. & Diniz, P. S. R. (2001). Adaptive RFI cancellation in VDSL systems. *European Conf. on Circuit Theory and Design (ECCTD'01)*, Espoo, Finland, pp. III-217-III-220, 28-31 Aug. 2001.


**Digital Filters**

Edited by Prof. Fausto Pedro GarcÃa MÃ¡rquez

ISBN 978-953-307-190-9
Hard cover, 290 pages
**Publisher** InTech
**Published online** 11, April, 2011
**Published in print edition** April, 2011

The new technology advances provide that a great number of system signals can be easily measured with a low cost. The main problem is that usually only a fraction of the signal is useful for different purposes, for example maintenance, DVD-recorders, computers, electric/electronic circuits, econometric, optimization, etc. Digital filters are the most versatile, practical and effective methods for extracting the information necessary from the signal. They can be dynamic, so they can be automatically or manually adjusted to the external and internal conditions. Presented in this book are the most advanced digital filters including different case studies and the most relevant literature.

**How to reference**

In order to correctly reference this scholarly work, feel free to copy and paste the following:

Zlatka Nikolova, Georgi Stoyanov, Georgi Iliev and Vladimir Poulkov (2011). Complex Coefficient IIR Digital Filters, Digital Filters, Prof. Fausto Pedro GarcÃa MÃ¡rquez (Ed.), ISBN: 978-953-307-190-9, InTech, Available from: http://www.intechopen.com/books/digital-filters/complex-coefficient-iir-digital-filters

INTECH
open science | open minds

**InTech Europe**
University Campus STeP Ri
Slavka Krautzeka 83/A
51000 Rijeka, Croatia
Phone: +385 (51) 770 447
Fax: +385 (51) 686 166
www.intechopen.com

**InTech China**
Unit 405, Office Block, Hotel Equatorial Shanghai
No.65, Yan An Road (West), Shanghai, 200040, China
中国上海市延安西路65号上海国际贵都大饭店办公楼405单元
Phone: +86-21-62489820
Fax: +86-21-62489821